Taylor & Francis
Taylor & Francis Group

Journal of Computational and Theoretical Transport

ISSN: 2332-4309 (Print) 2332-4325 (Online) Journal homepage: www.tandfonline.com/journals/ltty21

A Stable Wavelet Computational Method for the Study of Generalized Burger–Fisher and Burgers–Huxley Models

Aslam Khan , Abdul Ghafoor , Kamal Shah , Thabet Abdeljawad & Manar A. Alqudah

To cite this article: Aslam Khan , Abdul Ghafoor , Kamal Shah , Thabet Abdeljawad & Manar A. Alqudah (2025) A Stable Wavelet Computational Method for the Study of Generalized Burger–Fisher and Burgers–Huxley Models, Journal of Computational and Theoretical Transport, 54:6-7, 436-461, DOI: 10.1080/23324309.2025.2580614

To link to this article: https://doi.org/10.1080/23324309.2025.2580614

JOURNAL OF COMPUTATIONAL AND THEORETICAL TRANSPORT
2025, VOL. 54, NOS. 6–7, 436–461
https://doi.org/10.1080/23324309.2025.2580614

Taylor & Francis
Taylor & Francis Group

A Stable Wavelet Computational Method for the Study of Generalized Burger–Fisher and Burgers–Huxley Models

Aslam Khan[a], Abdul Ghafoor[a], Kamal Shah[b,c], Thabet Abdeljawad[b,d,e,f], and Manar A. Alqudah[g]

[a]Institute of Numerical Sciences, Kohat University of Science and Technology, Kohat, Pakistan; [b]Department of Mathematics and Sciences, Prince Sultan University, Riyadh, Saudi Arabia; [c]Department of Mathematics, University of Malakand, Chakdara Dir(L), Pakistan; [d]Department of Fundamental Sciences, Faculty of Engineering and Architecture, Istanbul Gelisim University, Avcilar, Istanbul, Turkey; [e]Department of Medical Research, China Medical University, Taichung, Taiwan; [f]Department of Mathematics and Applied Mathematics, School of Science and Technology, Sefako Makgatho Health Sciences University, Ga-Rankuwa, South Africa; [g]Department of Mathematical Sciences, College of Sciences, Princes Nourah bint Abdulrahman University, Riyadh, Saudi Arabia

ABSTRACT

This work proposes, a hybrid numerical scheme to study the generalized Burger–Fisher equation (gBFE) and generalized Burgers-Huxley equation (gBHE). This strategy comprises Haar wavelet and Runge-Kutta (RK-4) routine solver. We use the collocation approach to approximate the unknown solution and derivatives at discrete points, reducing the given problem to its corresponding nonlinear initial value problem. Then, an efficient time integration scheme is used to solve the consequent system. The proposed technique is implemented for the numerical simulations of various problems that includes gBFE and gBHE. To further elaborate the efficiency of the scheme, L_2, L_∞ and L_{rms} error measures are computed. The computed results are also compared with some existing results in literature. It is observed that the proposed scheme is quite good for the numerical solutions of the gbFE and gBHE model equations. Besides this, the computational stability of the proposed method is examined *via* the eigenvalues procedure.

KEYWORDS

Haar wavelet; RK-4 solver; nonlinear equations; stability analysis

1. Introduction

Numerous reaction-diffusion mechanisms in various areas of engineering and sciences can be formulated in terms of nonlinear partial differential equations (NPDEs). Due to these widespread applications of NPDEs, many researchers are attracted to explore the solutions of NPDEs. Amongst NPDEs, one of the famous nonlinear model is described below:

CONTACT Abdul Ghafoor abdulghafoor@kust.edu.pk Institute of Numerical Sciences, Kohat University of Science and Technology, Kohat, KP 26000, Pakistan; Thabet Abdeljawad tabdeljawad@psu.edu.sa Department of Mathematics and Sciences, Prince Sultan University, Riyadh, Saudi Arabia.

$$\mathcal{W}_t + \alpha \mathcal{W}^{\sigma} \mathcal{W}_{\xi} - \gamma \mathcal{W}_{\xi\xi} = \beta F(\mathcal{W}), \xi \in \Theta, t > 0, \tag{1.1}$$

where $\Theta = [a, b] \subseteq R$, $\mathcal{W} = \mathcal{W}(\xi, t)$, $F(\mathcal{W})$ is the non-linear expression and $\alpha \geq 0$, $\sigma \geq 1$, $\gamma, \beta > 0$. The corresponding initial and boundary conditions are:

$$\mathcal{W}(\xi, 0) = h_0(\xi), \xi \in \Theta, \tag{1.2}$$

$$\mathcal{W}(a, t) = g_1(t), \mathcal{W}(b, t) = g_2(t), t > 0, \tag{1.3}$$

where h_0 represents the initial condition, whereas, g_1 and g_2 denote left and right boundary conditions, respectively. From Equation (1.1), one can extract the following well-known models that describe the population evolution of two parallel mechanisms namely: nonlinear local multiplication and diffusion (Mittal and Arora 2010; Mittal and Jiwari 2009).

1.1. Generalized Burger–Fisher equation

The gBFE has many applications in plasma physics, fluid mechanics, and elasticity (Mittal and Rohila 2017). This model is highly nonlinear, and the analytical ways are quite limited in determining its closed form solution. Therefore, to overcome with this issue, numerical strategies are essential in the solution procedures. Several numerical techniques have been addressed for the solutions of gBFE in the previous work. For instance, Sari, Gürarslan, and Dağ (2010) solved gBFEs using hybrid scheme based on sixth-order finite difference method (FDM) and third-order total variation diminishing Runge Kutta. Bratsos (2013) developed an improved FDM with modified predictor-corrector numerical scheme for gBFEs. Pirdawood and Sabawi solved gBFEs numerically *via* compact numerical scheme based on fourth-order FDM and diagonal implicit Runge Kutta method (Pirdawood and Sabawi 2021). Sari, Gürarslan, and Dağ (2010), Bratso (Bratsos 2013), Pirdawood and Sabawi (Pirdawood and Sabawi 2021) employed FDM to solve the underlying problem. FDM works well for those problem having regular geometry. However, it lacks flexibility in case of irregular domain problems. Javidi (2006) proposed spectral collocation based method for the numerical solutions of gBFEs. Spectral methods are typically well-suited for problems with simple problem. Zhao et al. (2012) applied Chebyshev-Legendre pseudo-spectral method to solve gBFE. Spectral methods have exponential convergence for smooth problems, achieves high precision with few nodal points, and are well suited for periodic domains. However, these methods underperformed for problems with non-smoothness and complex geometries. Zhu and Kang (2010) implemented Quasi-interpolation cubic b-spline along with collocation technique. For problems with irregular grids and complex geometries, spline methods perform very well. Higher order splines deliver high accuracy with fewer

nodes as compared to FDM. However, their convergence rate is only algebraic, imposing higher order boundary conditions can be nontrivial, and are computationally expensive methods. Malik et al. (2015) suggested a hybrid algorithm *via* an exponential function coupled with heuristic computation that converts the given NPDEs to the nonlinear ordinary differential equations (NODEs). The strength of hybrid method lies in its robustness, accuracy, and capability to tackle nonlinear complex models. However, they are computationally expensive, and convergence is not guaranteed. Also, the NODEs were transformed to an optimization problem, estimating some unknown parameters which makes the processes complicated. In light of the above discussion and literature review, it is clear that each numerical scheme has its advantages and limitations. For further analysis, the interested readers are referred to see (Singh, Dahiya, and Singh 2020; Hussain and Haq 2021; Mittal and Tripathi 2015; Mujahid and Mehnaz 2016; Rashidi, Ganji, and Dinarvand 2009; Xu and Xian 2010; Akinfe and Loyinmi 2021; Wasim, Abbas, and Amin 2018; Fatima 2022).

1.2. Generalized Burger–Huxley equation

When $F(\mathcal{W}) = \mathcal{W}(1-\mathcal{W}^{\sigma})(\mathcal{W}^{\sigma}-\eta), 0 < \eta < 1$, then Equation (1.1) represents the generalized Burger-Huxley equation (gBHE). This model explains the dynamics of various nonlinear physical phenomena, like the archetype models relating the interaction of reaction, convection and diffusion mechanisms (Ablowitz, Fuchssteiner, and Kruskal 1987). In existing literature, some remarkable applications of these models have been reported in combustion, chemistry, metallurgy and engineering, among others (Singh, Arora, and Singh 2016) and so on. Various studies suggested numerical techniques for the solutions of gBHE. Singh, Arora, and Singh (2016) applied modified cubic b-spline differential quadrature procedure to solve gBHE. Along the similar lines, Bratsos (2011) implemented fourth order scheme to solve gBHE. Verma and Kayenat (Verma and Kayenat 2020) proposed efficient Mickens' type NSFD technique to solve gBHE. Darvishi, Kheybari, and Khani (2008) developed spectral collocation technique and dervishis preconditionings to solve gBHE. Çelik (2016) proposed collocation method based on Chebyshev wavelet for the solution of gBHE. Sari and Gürarslan (2009) utilized differential quadrature schemes. For more existing numerical techniques, the readers are referred to check (Inan and Bahadir 2015; Az-Zo'bi 2014; Shiralashetti and Kumbinarasaiah 2018; Machado, Babaei, and Moghaddam 2016; Kumar, Yadav, and Nagar 2022; Çelik 2012; Zaman et al. 2024; Ali Shah et al. 2023).

In the context of our work, both gBFE and gBHE are highly nonlinear models due to the presence of nonlinear convection and diffusion terms, hence, making an analytical solution quite impossible except for some cases

in which approximations have been used to relaxe the coupling terms. Taking into account slow fast dynamics add more complexity to the system and thus numerical solutions are viable approaches to tackle with such complicated model equations. In few of our test problems, we analyze the solution of model having slow-fast kinetics.

Recently, wavelets numerical strategies attained prominent devotion. Wavelets are characterized by key properties: orthogonality, compact support, and regularity. Consequently, they have been frequently employed for the numerical ODEs, PDEs, and integral equations (Lepik 2005; Lepik 2011; Ghafoor, Haq, et al. 2022; Ghafoor, Haq, et al. 2022; Haq and Ghafoor 2018; Maleknejad, Lotfi, and Mahdiani 2007). In all wavelet kinfolks, Haar wavelet (HW) deserves considerable curiosity. HW depends on Haar functions, which were first investigated by Alfr $\acute{e}$ d Haar (Farkov et al. 2019). These wavelets are discrete in nature, that give the output values $-1, 0,$ and 1. The output constant values also leads to differentiability problems at the end points of the intervals which is one of the drawbacks of these HW.

To deal with this issue, it would be interesting to apply the integral approach rather than the differential approach. Hybrid HW methods have been used extensively in the literature to solve nonlinear model equations. These hybrid methods include the HW approach integrated with the finite difference method. While using these hybrid methods to solve evolutionary models, accurate results have been reported. However, using these methods also have some down sides. First, to solve the time-dependent PDEs in the extended domains, one has to transform the interval to the [0, 1] while using these methods. This transformation is inevitable for the solution. With this transformation, accuracy is quite affected. Second, these hybrid methods uses linearization techniques in order to linearize the nonlinear terms in the model. These linearization techniques also affect the solution accuracy. Therefore, the primary goal of the new numerical technique is to reduce computational cost and address the drawbacks present in existing methods.

In this work, we construct a new strategy based on HW and ordinary differential equations solver to visualize the numerical view of gBFEs and gBHEs models. To the best our knowledge, the proposed work is novel and so far not reported for the solutions of the mentioned models in literature.

The rest of the paper is organized as follows:

- The fundamental preliminaries are given in Section 2
- The proposed numerical strategy and the computed outcomes are presented in Sections 3 and 4, respectively
- The computational stability of the proposed scheme is reported in Section 5
- Finally, the conclusions are drawn in Section 6.

2. Preliminaries

In this part of the manuscript, some elementary results associated with the present work are described.

2.1. HW and its integrals

Let $[a, b)$ is an arbitrary domain. Assume $d\xi = \frac{b-a}{2C}$, where $C = 2^J$, and J represents the maximum level of resolution, to segregate the interval $[a, b)$ into 2C equal sub-intervals. Also, define $\lambda = 0, 1, 2, ..., C$, $\ell = 0, 1, 2, ..., 2^{\lambda} - 1$, $i = c + \ell + 1$ and $c = 2^{\lambda}$, which describe the dilation parameter, translation parameter and the wavelet number, respectively. The first 1^{st} and j^{th} order HW are defined as (Lepik 2011):

$$h_1(\xi) = \begin{cases} 1, & \xi \in [a, b), \\ 0, & \text{elsewhere}, \end{cases} \tag{2.1}$$

$$h_j(\xi) = \begin{cases} 1 & \xi \in [\varsigma_1(j), \varsigma_2(j)), \\ -1, & \xi \in [\varsigma_2(j), \varsigma_3(j)), \\ 0, & \text{elsewhere}, \end{cases} \tag{2.2}$$

where $\varsigma_1(e) = a + (2\ell)vd\xi, \varsigma_2(j) = a + (2\ell + 1)vd\xi, \varsigma_3(j) = a + 2(\ell + 1)vd\xi$, and $v = \frac{C}{c}$. Since, HW are piecewise constant functions and are not differentiable at the end points of the sub interval. Therefore, we will utilize the integral approach, and these integrals appear in repeated form as:

$$I_{j,m}(s) = \int_a^{\xi} \int_a^{\xi} \dots \int_a^{\xi} h_j(z) dz^m = \frac{1}{(m-1)!} \int_a^{\xi} (\xi - z)^{m-1} h_j(z) dz, \tag{2.3}$$

where $m = 1, ..., n$ (order of the spatial derivative), $j = 1, ..., 2C$. Now, collectively Equations (2.1) and (2.2), and Equation (2.3) gives the following formulae:

$$Z_{1,m}(\xi) = \frac{(\xi - a)^m}{m!}, \tag{2.4}$$

$$Z_{j,m}(\xi) = \begin{cases} 0, & \xi < \varsigma_1(j), \\ \frac{1}{m!}\left[\xi - \varsigma_1(j)\right]^m, & \xi \in \left[\varsigma_1(j), \varsigma_2(j)\right], \\ \frac{1}{m!}\left[(\xi - \varsigma_1(j))^m - 2(\xi - \varsigma_2(j))^m\right], & \xi \in \left[\varsigma_2(j), \varsigma_3(j)\right], \\ \frac{1}{m!}\left[(\xi - \varsigma_1(j))^m - 2(\xi - \varsigma_2(j))^m + (\xi - \varsigma_3(j))^m\right], & \xi > \varsigma_3(j). \end{cases} \tag{2.5}$$

2.2. Function estimation

Since, HW form basis therefore, it can used to estimate a square integrable function in an interval $[a, b)$ as:

$$\mathcal{W}(\xi) = \sum_{j=1}^{\infty} \lambda_j h_j(\xi), \tag{2.6}$$

where λ_j are the unknown wavelets coefficients to be determined *via* interpolation condition. As the series extends up to infinity, and we need the finite terms for numerical computations that is why one can use the finite term approximations described below:

$$\mathcal{W}(\xi) = \sum_{j=1}^{2C} \lambda_j(t) h_j(\xi) + O(h_j^{2C+1}). \tag{2.7}$$

Neglecting the involved error term we have:

$$\mathcal{W}(\xi) = \sum_{j=1}^{2C} \lambda_j(t) h_j(\xi) = \mathrm{S}^T(t)\mathrm{H}(\xi), \tag{2.8}$$

where $\mathrm{S}^T(t) = [\lambda_1, \lambda_2, \lambda_3, ..., \lambda_{2C}]$, $\mathrm{H}(\xi) = [h_1(\xi), h_2(\xi), h_3(\xi), ..., h_{2C}(\xi)]^T$, and T denotes the transpose.

2.3. Time marching scheme

Here, we recall the time marching Runge-Kutta method (RK − 4), which is defined as follows:

$$\begin{aligned}
&\mathrm{K}_1 = \mathrm{H}(t^n, \mathcal{W}^n),\\
&\mathrm{K}_2 = \mathrm{H}\left(t^n + \frac{\partial t}{2}, \mathcal{W}^n + \frac{\mathrm{K}_1}{2}\right),\\
&\mathrm{K}_3 = \mathrm{H}\left(t^n + \frac{\partial t}{2}, \mathcal{W}^n + \frac{\mathrm{K}_2}{2}\right),\\
&\mathrm{K}_4 = \mathrm{H}(t^n + \partial t, \mathcal{W}^n + \mathrm{K}_3),\\
&\mathcal{W}^{n+1} = \mathcal{W}^n + \frac{\partial t}{6}(\mathrm{K}_1 + 2(\mathrm{K}_2 + \mathrm{K}_3) + \mathrm{K}_4), n = 0, 1, 2, ..., \text{ and } \partial t \text{ is the time step size.}
\end{aligned} \tag{2.9}$$

3. Proposed numerical strategy

Here, the proposed numerical technique is presented. First, we discretize the solutions and the spatial derivatives at discrete points *via* HW basis which transforms the system to nonlinear initial value problem. Then, the

solutions at arbitrary time can be extracted using an ODEs solver. Here, we use the RK-4 algorithm. Since HW has differentiability issues at the end points of each sub interval, therefore, an integral approach is employed. In this approach, the highest order derivative is estimated with HW series while lower order derivative and the unknown function can be approximated with successive integration. Here, we consider derivative approximation in Equation (1.1) as:

$$\mathcal{W}_{\xi\xi}(\xi,t)=\sum_{j=1}^{2C}\lambda_j(t)h_j(\xi). \tag{3.1}$$

Integration from a to ξ gives:

$$\int_a^{\xi}\mathcal{W}_{\tilde{\xi}}(\tilde{\xi},t)d\tilde{\xi}=\int_a^{\xi}(\sum_{j=1}^{2C}\lambda_j(t)h_j(\tilde{\xi}))d\tilde{\xi}=\sum_{j=1}^{2C}\lambda_j(t)\mathrm{Z}_{j,1}(\xi)+\mathcal{W}_{\xi}(\xi,t)|_{\xi=a}, \tag{3.2}$$

where $\int_a^{\xi}h_j(\tilde{\xi})d\xi=\mathrm{Z}_{j,1}(\xi)$. Similarly, we have:

$$\mathcal{W}(\xi,t)=\sum_{j=1}^{2C}\lambda_j(t)\mathrm{Z}_{j,2}(\xi)+(\xi-a)(\mathcal{W}_{\xi}(\xi,t))|_{\xi=a}+\mathcal{W}(\xi,t)|_{\xi=a}. \tag{3.3}$$

From Equations (3.2)–(3.3) one can obtain:

$$\mathcal{W}_{\xi}(\xi,t)|_{\xi=a}=\frac{g_2(t)-g_2(t)}{b-a}-\frac{1}{b-a}\sum_{j=1}^{2C}\lambda_j(t)\mathrm{Z}_{j,2}(b). \tag{3.4}$$

Incorporating Equation (3.4) in Equation (3.2) and Equation (3.3) the obtained results are given by:

$$\mathcal{W}_{\xi}(\xi,t)=\sum_{j=1}^{2C}\lambda_j(t)\left[\mathrm{Z}_{j,1}(\xi)-\frac{1}{b-a}\mathrm{Z}_{j,2}(b)\right]+\frac{g_2(t)-g_1(t)}{b-a}, \tag{3.5}$$

$$\mathcal{W}(\xi,t)=\sum_{j=1}^{2C}\lambda_j(t)\left[\mathrm{Z}_{j,2}(\xi)-\frac{\xi-a}{b-a}\mathrm{Z}_{j,2}(b)\right]+\frac{\xi-a}{b-a}g_2(t)+\frac{b-\xi}{b-a}g_2(t). \tag{3.6}$$

At $\xi=\xi_m$, Equation (3.1) and Equations (3.5)–(3.6), can be expressed as:

$$\mathcal{W}_{\xi\xi}(\xi,t)=\mathcal{H}\mathrm{S}(t), \tag{3.7}$$

$$\mathcal{W}_{\xi}(\xi,t)=\mathcal{M}_{\mathbf{1}}\mathrm{S}(t)+\mathcal{N}_{\mathbf{1}}(t), \tag{3.8}$$

$$\mathcal{W}(\xi,t)=\mathcal{M}_{\mathbf{0}}\mathrm{S}(t)+\mathcal{N}_{\mathbf{0}}(t), \tag{3.9}$$

where

$$\mathcal{M}_{\mathbf{1}} = \sum_{j=1}^{2C} \left[Z_{j,1}(\xi_m) - \frac{1}{b-a} Z_{j,2}(b) \right], \mathcal{N}_{\mathbf{1}}(t) = \frac{g_2(t) - g_1(t)}{b-a},$$

$$\mathcal{M}_{\mathbf{0}} = \sum_{j=1}^{2C} \left[Z_{j,2}(\xi_m) - \frac{\xi_m - a}{b-a} Z_{j,2}(b) \right], \mathcal{N}_{\mathbf{0}}(t) = \frac{\xi_m - a}{b-a} g_2(t) + \frac{b-\xi_m}{b-a} g_1(t).$$

Substitution of Equations (3.7)–(3.9) in Equation (1.1), one can obtain the following coupled equations:

$$\frac{d\mathcal{W}}{dt} = \gamma[\mathcal{H}S(t)] - \alpha\left[\mathcal{M}_{\mathbf{0}}S(t) + \mathcal{N}_{\mathbf{0}}(t)\right]^{\sigma} * \left[\mathcal{M}_{\mathbf{1}}S(t) + \mathcal{N}_{\mathbf{1}}(t)\right] + \beta F\left[\mathcal{M}_{\mathbf{0}}S(t) + \mathcal{N}_{\mathbf{0}}(t)\right], \tag{3.10}$$

where '*' represent the element wise product of two vectors. Equation (3.10) represents the system of initial valued problems that can be solved by built in MATLAB routine package that uses the explicit RK-4 technique.

4. Numerical results and discussion

Here, to testify the proposed scheme, the numerical solutions of gBFE and gBHE are reported. To measure the effectiveness of the results, we use the L_2, L_∞ and L_{rms} norms which are presented below:

$$L_2 = \| \mathcal{W}^E - \mathcal{W}^N \|_2 \cong \sqrt{d\xi \sum_{e=1}^{2C} |\mathcal{W}_e^E - \mathcal{W}_e^N|^2}, \tag{4.1}$$

$$L_\infty = \| \mathcal{W}^E - \mathcal{W}^N \|_\infty \cong max_\infty |\mathcal{W}_e^E - \mathcal{W}_e^N|, \tag{4.2}$$

$$L_{rms} = \sqrt{\sum_{e=1}^{2C} \left(\frac{\mathcal{W}^E - \mathcal{W}^N}{\sqrt{2C}} \right)^2}, \tag{4.3}$$

where $\mathcal{W}^E$ and $\mathcal{W}^N$ represent the exact and numerical solutions.

4.1. Problem 1

First, we consider gBFE (Equation (1.1)) for $\gamma = 1$ and $\rho = 1$ with closed form solution described below:

$$\mathcal{W}(\xi, t) = \left[\frac{1}{2} + \frac{1}{2} \tanh(m_1(\xi - m_2 t)) \right]^{\frac{1}{\sigma}}, \tag{4.4}$$

where

$$m_1 = \frac{-\sigma\alpha}{2(1+\sigma)}, \quad m_2 = \frac{\alpha}{1+\sigma} + \frac{\beta(1+\sigma)}{\alpha}.$$

The associated initial and boundary conditions are extracted from the closed form solution. For the analysis and comparison with other numerical techniques, the given problem is solved in different spatial domain with various parameters with total time, $t = 20$. We describe the simulation results of problem 1 in the following cases.

Initially, the stated problem is solved in the spatial domain *[0, 1]* with different parameters. Details of each computational experiment for various parameters of interest are as follows: The parameters used for this case are $\alpha = 1 = \beta$ and different value of σ, particularly 1, 4, 8 (case 1.1). The obtained error norms and computational time are listed in the Table 1 for $t = 0.3, 0.9$. Similarly, the numerical simulations are performed with $\alpha = 0.1$, $\beta = -0.25$ and $\sigma = 01, 04, 08$ (case 1.2). In Table 2, the obtained maximum error norms and computational time are listed for different times $t = 0.3, 0.9$. Next, for the comparison purpose, the corresponding problem is solved in the spatial domain $\xi \in [-1, 1]$ with different values of parameter. First, we set parameters $\alpha = \beta = \sigma = 1$ (case 1.3), for numerical computation up to final time $t = 20$. Finally, we set $\alpha = \beta = 1$, $\sigma = 2$ (case 1.4). The obtained error norms are listed for both set of parameters in Table 3. In all experiments, the obtained results are matched with the reference work

Table 1. Corresponding different error norms between exact and numerical of problem 1 (case 1.1).

		Proposed method		MQ (Hussain and Haq 2021)		Gs (Hussain and Haq 2021)		Computational
t	σ	L_∞	L_{rms}	L_∞	L_{rms}	L_∞	L_{rms}	time (s)
0.3	01	5.765×10^{-8}	3.791×10^{-8}	1.347×10^{-4}	8.046×10^{-5}	2.399×10^{-3}	1.131×10^{-3}	0.856072
	04	1.062×10^{-7}	7.135×10^{-8}	2.778×10^{-3}	1.932×10^{-3}	3.089×10^{-3}	1.695×10^{-3}	0.921262
	08	1.123×10^{-7}	7.514×10^{-8}	9.985×10^{-4}	6.964×10^{-4}	1.045×10^{-3}	5.540×10^{-4}	0.892620
0.9	01	1.861×10^{-8}	1.250×10^{-8}	2.186×10^{-3}	1.520×10^{-3}	9.025×10^{-3}	4.493×10^{-3}	1.983624
	04	4.592×10^{-8}	3.041×10^{-8}	5.708×10^{-4}	3.986×10^{-4}	2.247×10^{-3}	1.188×10^{-3}	1.986794
	08	1.861×10^{-9}	1.224×10^{-9}	1.080×10^{-5}	7.558×10^{-6}	1.422×10^{-4}	9.990×10^{-5}	1.908212

Table 2. Computed maximum error norm between exact and numerical solution of problem 1 (case 1.2).

		Proposed method	MQ (Hussain and Haq 2021)	Gs (Hussain and Haq 2021)	S3 (Hussain and Haq 2021)	Computational
t	σ	L_∞	L_∞	L_∞	L_∞	time (s)
0.3	01	2.904×10^{-8}	3.863×10^{-6}	1.632×10^{-7}	4.942×10^{-5}	0.977598
	04	5.190×10^{-8}	2.531×10^{-5}	1.880×10^{-7}	4.419×10^{-4}	0.944732
	08	5.940×10^{-8}	1.858×10^{-5}	1.732×10^{-7}	1.038×10^{-3}	0.918772
0.9	01	3.050×10^{-8}	9.481×10^{-6}	2.754×10^{-7}	2.980×10^{-4}	2.188532
	04	6.431×10^{-8}	1.062×10^{-5}	4.091×10^{-7}	3.456×10^{-3}	2.172652
	08	8.407×10^{-8}	2.387×10^{-6}	3.740×10^{-7}	1.220×10^{-2}	2.212019

Table 3. Obtained different error norms between exact and numerical solution of problem 1 (case 1.3).

	Proposed method			MQ (Hussain and Haq 2021)			(Mittal and Tripathi 2015)	
t	L_∞	L_2	L_{rms}	L_∞	L_2	L_{rms}	L_∞	L_2
Case 1.3								
0.5	9.595×10^{-8}	5.481×10^{-7}	6.215×10^{-8}	1.626×10^{-2}	1.662×10^{-2}	1.147×10^{-3}	9.172×10^{-6}	6.952×10^{-6}
1	8.359×10^{-8}	4.954×10^{-7}	5.685×10^{-8}	8.085×10^{-3}	8.252×10^{-3}	5.694×10^{-3}	6.852×10^{-6}	6.13×10^{-6}
2	1.480×10^{-7}	8.630×10^{-7}	9.838×10^{-8}	1.136×10^{-3}	1.155×10^{-3}	7.970×10^{-4}	7.304×10^{-6}	7.228×10^{-6}
4	3.298×10^{-8}	1.882×10^{-7}	2.128×10^{-8}	7.998×10^{-6}	8.797×10^{-6}	6.071×10^{-6}	6.443×10^{-7}	6.702×10^{-7}
20	5.550×10^{-13}	3.265×10^{-12}	3.845×10^{-13}	2.398×10^{-14}	1.992×10^{-14}	1.374×10^{-14}	–	–
Case 1.4								
1	1.942×10^{-7}	1.139×10^{-6}	1.302×10^{-7}	2.284×10^{-3}	2.322×10^{-3}	1.602×10^{-3}	–	–
5	1.047×10^{-10}	5.934×10^{-10}	6.686×10^{-11}	1.447×10^{-7}	1.480×10^{-7}	1.021×10^{-7}	2.139×10^{-6}	1.189×10^{-6}
10	2.666×10^{-13}	1.542×10^{-12}	1.756×10^{-13}	2.16×10^{-12}	2.208×10^{-12}	1.524×10^{-12}	2.139×10^{-6}	1.189×10^{-6}
15	1.387×10^{-12}	8.242×10^{-12}	9.470×10^{-13}	2.142×10^{-14}	2.269×10^{-14}	1.566×10^{-14}	2.138×10^{-6}	1.188×10^{-6}
20	1.388×10^{-12}	8.250×10^{-12}	9.480×10^{-13}	2.309×10^{-14}	2.453×10^{-14}	1.693×10^{-14}	2.138×10^{-6}	1.187×10^{-6}

Table 4. Corresponding various error norms between exact and numerical solution of problem 1.

Cases	t	L_∞	L_2	L_{rms}
Case 1.5	0.5	8.996×10^{-5}	1.972×10^{-4}	2.093×10^{-7}
	1	1.330×10^{-4}	3.146×10^{-4}	6.870×10^{-7}
	2	1.487×10^{-4}	3.905×10^{-4}	3.066×10^{-6}
	4	1.771×10^{-4}	5.019×10^{-4}	2.470×10^{-5}
	10	2.557×10^{-5}	7.197×10^{-5}	4.552×10^{-6}
	20	1.388×10^{-9}	4.611×10^{-9}	2.315×10^{-10}
Case 1.6	1	1.105×10^{-4}	2.604×10^{-4}	2.103×10^{-6}
	5	1.529×10^{-4}	3.049×10^{-4}	7.330×10^{-6}
	10	3.868×10^{-7}	7.511×10^{-7}	3.326×10^{-8}
	15	8.925×10^{-12}	2.545×10^{-11}	1.222×10^{-12}
	20	2.766×10^{-12}	2.145×10^{-11}	2.660×10^{-12}

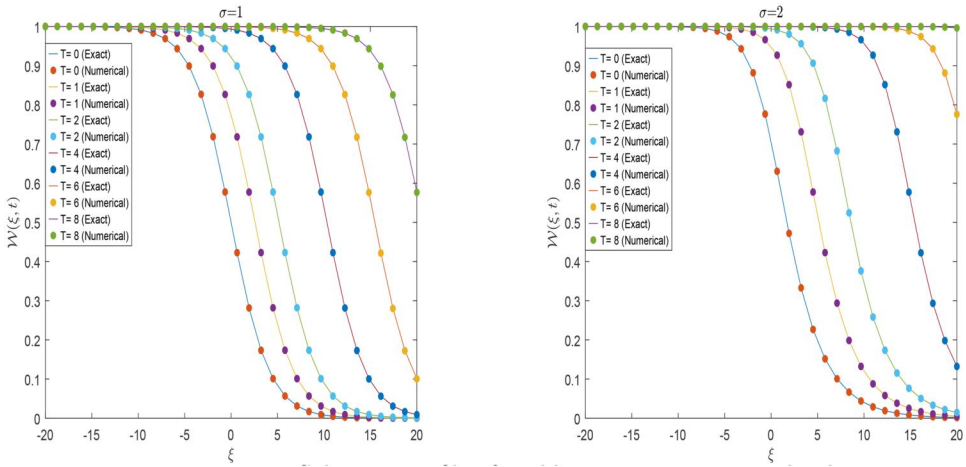

Figure 1. Solutions profile of problem 1 at various time levels.

(Hussain and Haq 2021; Mittal and Tripathi 2015). From the given results, it is evident that the results of the present scheme are highly accurate as compared to the cited work. Further, we elaborate the efficiency of the technique using spatial domain $[-20, 20]$ for the numerical simulations. In this case, numerical experiments are performed for the final time up to $t = 20$ with two set of parameters $\alpha = \beta = \sigma = 1$ (case 1.5) and $\alpha = \beta = 1$ and $\sigma = 2$ (case 1.6). The outcomes are presented in Table 4 for both set of parameters. The solutions profiles exact versus numerical are also plotted in Figure 1 for $\sigma = 1, 2$, which shows that both solutions are in good agreement.

4.2. Problem 2

Here, we take gBFE for $\gamma = \beta = 1$, $\alpha = 0$ and $\rho = 1$ with the following solution:

$$\mathcal{W}(\xi, t) = \left[\frac{1}{2} - \frac{1}{2}\tanh\left(\frac{\sigma}{2\sqrt{2\sigma+4}}\left[\xi - \left(\frac{\sigma+4}{\sqrt{2\sigma+4}}\right)t\right]\right)\right]^{\frac{2}{\sigma}}. \tag{4.5}$$

Table 5. Computed different error norms between analytical and numerical solution of problem 2.

	Proposed method			MQ (Hussain and Haq 2021)			Computational
t	L_∞	L_2	L_{rms}	L_∞	L_2	L_{rms}	time (s)
03	7.463×10^{-7}	3.082×10^{-6}	4.975×10^{-7}	4.258×10^{-4}	3.101×10^{-4}	3.026×10^{-4}	2.221082
04	3.592×10^{-7}	1.483×10^{-6}	2.395×10^{-7}	....	....	....	2.873438
05	1.629×10^{-7}	6.732×10^{-7}	1.086×10^{-7}	....	....	....	3.446513
10	2.607×10^{-9}	1.077×10^{-8}	1.739×10^{-9}	....	....	....	6.645378
15	4.045×10^{-11}	1.671×10^{-10}	2.698×10^{-11}	....	....	....	9.969633
20	6.271×10^{-13}	2.590×10^{-12}	4.183×10^{-13}	....	....	....	13.155609

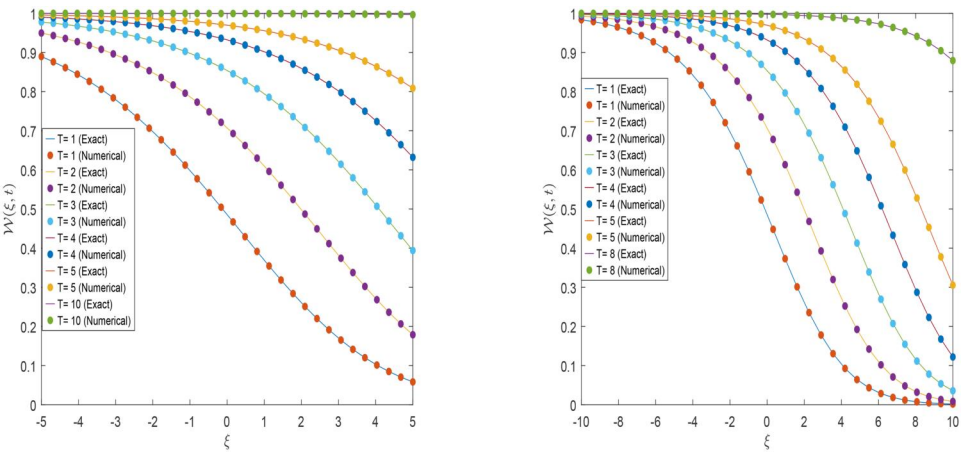

Figure 2. Solution profile of problem 2 at various time levels for $\xi \in [-5, 5]$ (left), $\xi \in [-10, 10]$ (right).

The necessary initial and boundary conditions are used from the given solution. For all computations of this problem we put $\sigma = 1$. The problem is solved in different spatial domains for maximum time up to $t = 20$. Simulations are carried out for testing and comparison purpose in the spatial domain $\xi \in [0, 1]$, and the obtained error norms are listed in Table 5 and computational time are also added in the same table. From table it is obvious that the present scheme produces good results as compared to the cited work and need less computational time. Geometrically, the solutions of this problem predict traveling wave behavior. To observe this behavior more clearly, the corresponding problem is also solved in spatial domains $[-5, 5]$ and $[-10, 10]$ respectively, and the results are displayed in Figure 2. In Table 6, the obtained error norms for the extended spatial domains are shown which reveals that the outcomes are also good if the domain is enlarged.

4.3. Problem 3

For $\alpha = 0$, $\gamma = \beta = \sigma = 1$ and $\rho = 2$, Equation (1.1) reduces to gBFE, with the following analytic solution:

Table 6. Obtained different error norms between exact and numerical solution of problem 2 in the extended spatial intervals.

Intervals	t	L_∞	L_2	L_{rms}
$\xi \in [-5, 5]$	01	4.004×10^{-5}	1.175×10^{-4}	1.333×10^{-5}
	02	6.926×10^{-5}	1.986×10^{-4}	2.392×10^{-5}
	03	4.798×10^{-5}	1.350×10^{-4}	1.753×10^{-5}
	04	1.616×10^{-5}	5.389×10^{-5}	8.052×10^{-6}
	05	8.332×10^{-6}	2.974×10^{-5}	4.558×10^{-6}
	10	4.786×10^{-7}	1.685×10^{-6}	2.550×10^{-7}
	15	8.858×10^{-9}	3.208×10^{-8}	4.919×10^{-9}
	20	1.419×10^{-10}	5.203×10^{-10}	8.022×10^{-11}
$\xi \in [-10, 10]$	01	1.221×10^{-4}	2.676×10^{-4}	7.443×10^{-6}
	02	2.037×10^{-4}	4.513×10^{-4}	1.837×10^{-5}
	03	2.083×10^{-4}	4.591×10^{-4}	2.876×10^{-5}
	04	1.435×10^{-4}	3.380×10^{-4}	3.689×10^{-5}
	05	1.217×10^{-4}	2.436×10^{-4}	2.658×10^{-5}
	10	6.570×10^{-6}	1.669×10^{-5}	1.996×10^{-6}
	15	2.063×10^{-7}	5.272×10^{-7}	6.188×10^{-8}
	20	3.492×10^{-9}	9.260×10^{-9}	1.114×10^{-9}

Table 7. Corresponding different error norms between exact and numerical solution of problem 3.

	Proposed method			MQ (Hussain and Haq 2021)			Computational
t	L_∞	L_2	L_{rms}	L_∞	L_2	L_{rms}	time (s)
0.1	7.247×10^{-8}	4.300×10^{-7}	4.935×10^{-8}	2.321×10^{-3}	1.657×10^{-3}	1.617×10^{-3}	0.216880
0.5	1.098×10^{-7}	6.391×10^{-7}	7.282×10^{-8}	9.628×10^{-4}	6.259×10^{-4}	6.108×10^{-4}	0.498917
1	9.177×10^{-8}	5.337×10^{-7}	6.079×10^{-8}	1.253×10^{-3}	8.464×10^{-4}	8.260×10^{-4}	0.827924
2	4.978×10^{-8}	2.896×10^{-7}	3.300×10^{-8}	4.341×10^{-3}	3.156×10^{-3}	3.080×10^{-3}	1.569856
3	2.557×10^{-8}	1.496×10^{-7}	1.708×10^{-8}	5.847×10^{-3}	4.263×10^{-3}	4.160×10^{-3}	2.116312

$$\varphi(x, t) = \frac{1}{1 + \exp[c_0(\xi - c_0 t)]}, \tag{4.6}$$

where c_0 is the known constant. The associated initial and boundary conditions are adjusted using analytical solution. First we solve the problem in the spatial domain $\xi \in [0, 1]$ to validate the scheme and compare the results with the existing numerical results in Table 7. The table also shows the execution time of the numerical experiment which show that the proposed solution method takes less computational time. The numerical results are computed for $c_0 = \frac{1}{\sqrt{2}}$ and for the final time up to 3, and presented in Table 8. It is apparently visible that our results are better from those described in Hussain and Haq (2021). Moreover, the numerical computations are also calculated in the spatial domain $[-10, 10]$ and $[-50, 50]$. In Figure 3 the achieved results are shown. The same figure also identifies the mutual comparison of exact and numerical solutions. Collectively, the graphical view show the method performance and traveling wave solutions. Besides this, in Table 9, the tabulated solutions are illustrated for various resolution levels and time. From table, it is clear when the resolution level raises, the accuracy increases.

Table 8. Computed different error norms of problem 3 at different time levels for $\xi \in [-10, 10]$.

t	L_∞	L_2	L_{rms}
0.1	3.127×10^{-6}	1.326×10^{-5}	2.105×10^{-8}
0.5	1.333×10^{-5}	5.556×10^{-5}	1.873×10^{-7}
1	2.306×10^{-5}	9.298×10^{-5}	6.150×10^{-7}
2	3.803×10^{-5}	1.444×10^{-4}	2.203×10^{-6}
3	5.031×10^{-5}	1.863×10^{-4}	4.548×10^{-6}

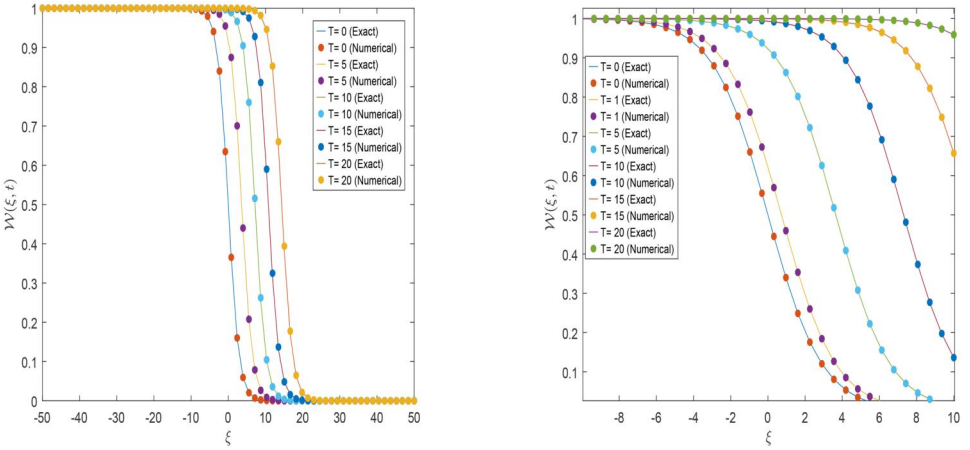

Figure 3. Solutions profile of problem 3 when $\xi \in [-50, 50]$ (left) and $\xi \in [-10, 10]$ (right).

4.4. Problem 4

In this case, we take the gBFE having no exact solution with $\alpha = 0$, $\gamma = 0.1$, $\beta = 1$, $\sigma = 1$ and $\rho = 1$. The boundary conditions are zero $\mathcal{W} = 0$ as $\xi \to \pm\infty$. The following two types of initial conditions are considered here:

$$h_0(\xi) = \begin{cases} \exp(7(\xi + 1)), & \xi < -1, \\ 1, & -1 \leq \xi \leq 1, \\ \exp(7(\xi + 1)), & \xi > 1, \end{cases} \tag{4.7}$$

and

$$h_0(\xi) = \operatorname{sech}(7\xi). \tag{4.8}$$

Numerical experiments are performed for the first type of initial condition Equation (4.7) in the spatial interval $[-4, 4]$ for the time $t = 0.5$ in first case (case 1.1). Similarly, the solutions are calculated in $[-10, 10]$ (case 1.2) for the final time $t = 5$. Graphical results are numerical plotted in Figure 4. In case 1.1, we noted that diffusion process dominant and the peaks stay near $\mathcal{W} = 1$. Similarly, the diffusion is also dominant up to $t = 0.5$ in case 1.2 but as the times increase the nonlinear reaction term dominates and the peaks in solution increases gradually reaching up to $\mathcal{W} = 1$. From both

Table 9. Obtained different error norms between exact and numerical solution of problem 3 for different level of resolution at different time levels when $\xi \in [0, 1]$.

t	J	L_∞	L_2	L_{rms}
0.1	1	3.579×10^{-6}	5.025×10^{-6}	2.303×10^{-6}
	2	1.003×10^{-6}	2.021×10^{-6}	6.474×10^{-7}
	3	2.981×10^{-7}	8.557×10^{-7}	1.941×10^{-7}
	4	1.170×10^{-7}	4.852×10^{-7}	7.844×10^{-8}
	5	7.247×10^{-8}	4.300×10^{-7}	4.935×10^{-8}
0.5	1	2.988×10^{-6}	4.049×10^{-6}	1.844×10^{-6}
	2	8.837×10^{-7}	1.737×10^{-6}	5.461×10^{-7}
	3	2.996×10^{-7}	8.380×10^{-7}	1.876×10^{-7}
	4	1.468×10^{-7}	5.977×10^{-7}	9.588×10^{-8}
	5	1.098×10^{-7}	6.391×10^{-7}	7.282×10^{-8}
1	1	1.881×10^{-6}	2.393×10^{-6}	1.059×10^{-6}
	2	4.719×10^{-7}	8.260×10^{-7}	2.364×10^{-7}
	3	6.487×10^{-8}	1.588×10^{-7}	1.116×10^{-8}
	4	5.410×10^{-8}	1.130×10^{-7}	1.004×10^{-8}
	5	1.177×10^{-8}	1.037×10^{-7}	1.001×10^{-8}
2	1	7.758×10^{-6}	1.166×10^{-5}	5.375×10^{-6}
	2	2.123×10^{-6}	4.372×10^{-6}	1.411×10^{-6}
	3	4.807×10^{-7}	1.393×10^{-6}	3.172×10^{-7}
	4	5.784×10^{-8}	2.338×10^{-7}	3.736×10^{-8}
	5	4.978×10^{-8}	2.896×10^{-7}	3.300×10^{-8}
3	1	7.825×10^{-6}	1.175×10^{-5}	5.414×10^{-6}
	2	2.164×10^{-6}	4.460×10^{-6}	1.414×10^{-6}
	3	5.087×10^{-7}	1.477×10^{-6}	3.368×10^{-7}
	4	8.179×10^{-8}	3.357×10^{-7}	5.404×10^{-8}
	5	2.557×10^{-8}	1.496×10^{-7}	1.708×10^{-8}

cases, it is noted that reaction diffusion term slowly effect the system. For the second type of initial condition Equation (4.8) the approximate solutions are computed over the spatial domains $[-4, 4]$ (case 1.1) and $[-10, 10]$ (case 1.2) for final time up to $t = 0.5$ and $t = 5$, respectively. Numerical measurements are shown in Figure 4. In case 1.1 the rapid decrease in the solutions peak is observed near $t = 0.5$ due to dominant diffusion term. However in case 1.2 as the time passes the peaks goes up and attain its maximum value at $t = 5$. From simulations, one can see that all the numerical solutions are perfectly matchable with the available results in the literature (Hussain and Haq 2021).

4.5. Problem 5

Taking $\alpha = 1$, and $\gamma = \sigma = \eta = 1$, Equation (1.1), reduces to the Huxley equation with exact solution given by:

$$\mathcal{W}(\xi, t) = \frac{1}{2} + \frac{1}{2}\tanh\left[\frac{1}{2\sqrt{2}}\left(\xi - \frac{1}{\sqrt{2}}t\right)\right], \quad t \geq 0. \tag{4.9}$$

This problem is numerically treated *via* the proposed method. For analysis and verifications of the results, two solutions domain [0, 1] and $[-50, 50]$ are used. The corresponding error norms in the interval [0, 1]

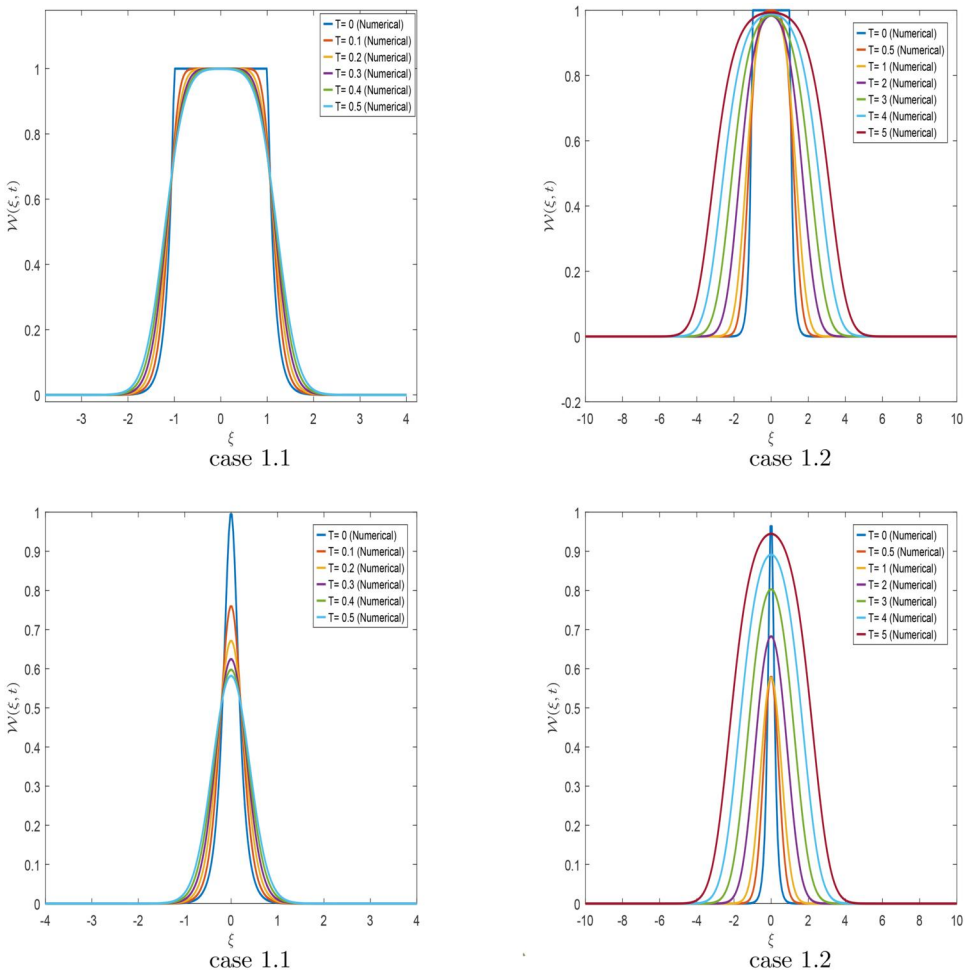

Figure 4. Physical behavior of the numerical solutions of problem 4.

at different times with varying resolution levels are listed in Table 10 while in Table 11, the same error norms are highlighted for the solution domain $[-50, 50]$. The tabulated data shows a concrete relation between the resolution level and accuracy which discloses the fact, that advancement in resolution level also enhances the accuracy. Another relation exists between the computational time and accuracy. More precisely this means when time increases the accuracy decreases due to round-off errors. The exact versus numerical measures are visualized in Figures 5 and 6. From figures the perfect match of both exact and numerical measures are visible.

4.6. Problem 6

Finally, we consider the gBHE given in Equation (1.1) with $\gamma = 1$, with closed form solution given by:

Table 10. Computed different error norms of problem 5 with different resolution levels.

t	J	L_∞	L_2	L_{rms}
0.1	1	3.579×10^{-6}	5.025×10^{-6}	2.303×10^{-6}
	3	2.981×10^{-7}	8.577×10^{-7}	1.941×10^{-7}
	6	6.160×10^{-8}	5.180×10^{-7}	4.207×10^{-8}
0.2	1	4.389×10^{-6}	6.227×10^{-6}	2.859×10^{-6}
	3	3.803×10^{-7}	1.089×10^{-6}	2.466×10^{-7}
	6	8.660×10^{-8}	7.178×10^{-7}	5.799×10^{-8}
0.4	1	3.694×10^{-6}	5.129×10^{-6}	2.348×10^{-6}
	3	3.471×10^{-7}	9.810×10^{-7}	2.208×10^{-7}
	6	9.976×10^{-8}	8.230×10^{-7}	6.637×10^{-8}
0.6	1	2.206×10^{-6}	2.868×10^{-6}	1.288×10^{-6}
	3	2.455×10^{-7}	9.810×10^{-7}	1.500×10^{-7}
	6	1.008×10^{-7}	8.314×10^{-7}	6.703×10^{-8}
0.8	1	5.450×10^{-7}	7.189×10^{-7}	1.171×10^{-7}
	3	1.362×10^{-7}	3.454×10^{-7}	7.003×10^{-8}
	6	9.940×10^{-8}	8.195×10^{-7}	6.606×10^{-8}
1	1	1.881×10^{-6}	2.393×10^{-6}	1.059×10^{-6}
	3	6.487×10^{-8}	1.588×10^{-7}	1.116×10^{-8}
	6	9.693×10^{-8}	7.989×10^{-7}	6.441×10^{-8}

Table 11. Obtained different error norms of problem 5 for different time levels.

t	L_∞	L_2	L_{rms}
0.1	1.896×10^{-5}	5.191×10^{-5}	7.493×10^{-9}
0.2	3.641×10^{-5}	9.895×10^{-5}	2.370×10^{-8}
0.3	5.231×10^{-5}	1.418×10^{-4}	4.964×10^{-8}
0.4	6.667×10^{-5}	1.810×10^{-4}	8.609×10^{-8}
0.5	7.952×10^{-5}	2.171×10^{-4}	1.336×10^{-7}
0.6	9.722×10^{-5}	2.504×10^{-4}	1.928×10^{-7}
0.7	1.057×10^{-4}	2.813×10^{-4}	2.638×10^{-7}
0.8	1.178×10^{-4}	3.100×10^{-4}	3.468×10^{-7}
0.9	1.289×10^{-4}	3.369×10^{-4}	4.419×10^{-7}
1	1.389×10^{-4}	3.621×10^{-4}	5.490×10^{-7}

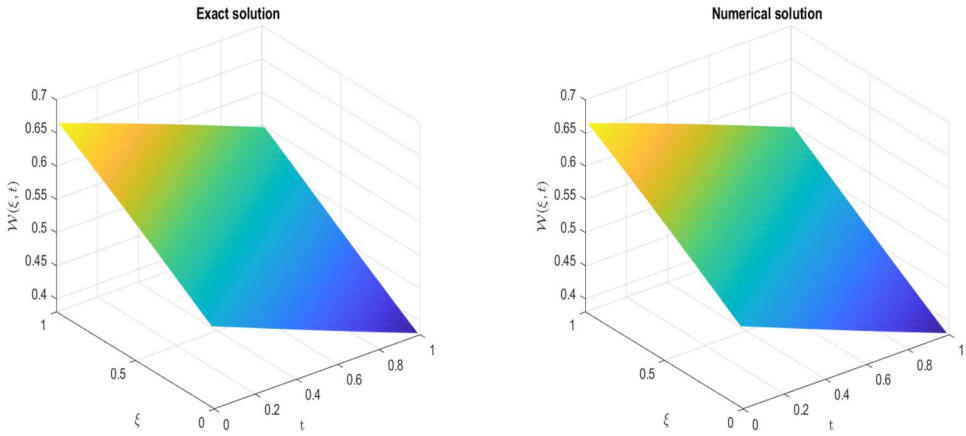

Figure 5. Exact versus numerical measures of problem 5.

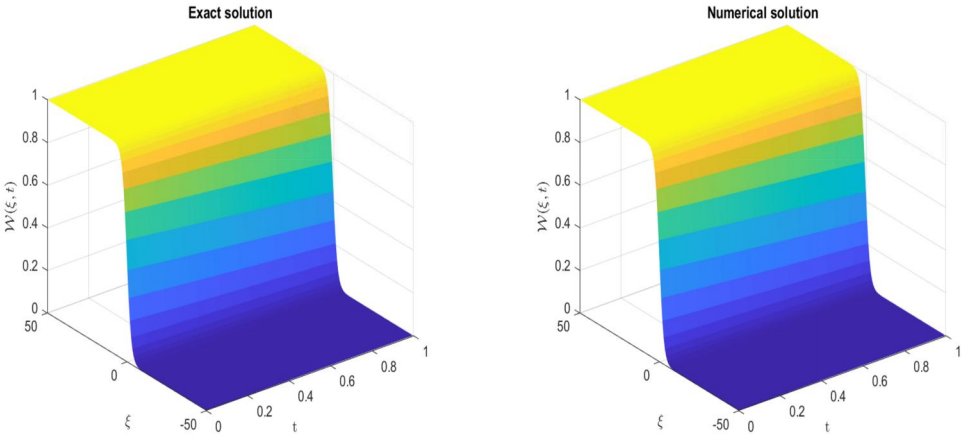

Figure 6. Exact and numerical measures of problem 5.

$$\mathcal{W}(x,t) = \left[\frac{1}{2} + \frac{1}{2}\tanh(\mathrm{V}_1(\xi - \mathrm{V}_2 t))\right]^{\frac{1}{\delta}}, t \geq 0, \tag{4.10}$$

where,

$$\mathrm{V}_1 = \frac{-\alpha\delta + \delta\sqrt{\alpha^2 + \beta(1+\delta)}}{4(1+\delta)}\delta,$$

$$\mathrm{V}_2 = \frac{\alpha\eta}{1+\delta} - \frac{(1+\delta-\eta)(-\alpha + \sqrt{\alpha^2 + 4\beta(1+\delta)})}{2(1+\delta)}.$$

The corresponding initial and boundary conditions are derived from the given solution. Numerical solutions are calculated for different parameters to compare the results with existing studies and also determine the solutions profile. Further, simulations are conducted for the following cases.

4.7. Case 1

In this case, the problem is treated for the spatial domain [0, 1]. The computational experiments are performed with the first set of parameters $\alpha = 1 = \beta$, $\eta = 0.001$ with different values of δ and $t = 0.2, 1$. Similarly, we take $\alpha = 0.1$, $\beta = 0.001$, $\eta = 0.0001$ and different value of δ at $t = 0.2, 1$ for further numerical experiments. Another set of parameters used for computations are $\alpha = 5$, $\delta = 1$ while varying β, η for time 0.3, 0.9. The outcomes of all set of parameters in terms of maximum error norms are recorded in Tables 12–14 and compared with Javidi and Golbabai (2009). From all tables, it is clear that computed solutions are in good agrement with the existing results in the previous study.

Table 12. Computed maximum error norm of problem 6 (case 1).

t	δ	Present	Algorithm 1 (Javidi and Golbabai 2009)	Algorithm 2 (Javidi and Golbabai 2009)	Algorithm 3 (Javidi and Golbabai 2009)
0.2	1	4.001×10^{-8}	4.129×10^{-8}	4.013×10^{-8}	4.013×10^{-8}
	4	1.309×10^{-5}	1.351×10^{-5}	1.313×10^{-5}	1.313×10^{-5}
	8	3.542×10^{-5}	3.656×10^{-5}	3.554×10^{-5}	3.554×10^{-5}
01	1	3.392×10^{-8}	4.685×10^{-8}	4.684×10^{-8}	4.684×10^{-8}
	4	1.526×10^{-5}	1.532×10^{-5}	1.532×10^{-5}	1.532×10^{-5}
	8	4.124×10^{-5}	4.140×10^{-5}	4.140×10^{-5}	4.140×10^{-5}

Table 13. Obtained maximum error norm between exact and numerical solution of problem 6 (case 1).

t	δ	Present	Algorithm 1 (Javidi and Golbabai 2009)	Algorithm 3 (Javidi and Golbabai 2009)	Algorithm 3 (Javidi and Golbabai 2009)
0.2	1	3.057×10^{-13}	3.156×10^{-13}	3.068×10^{-13}	2.992×10^{-13}
	4	5.689×10^{-10}	5.873×10^{-10}	5.710×10^{-10}	5.579×10^{-10}
	8	2.110×10^{-09}	2.178×10^{-9}	2.118×10^{-9}	2.075×10^{-9}
01	1	3.566×10^{-13}	3.586×10^{-13}	3.618×10^{-13}	3.142×10^{-13}
	4	6.637×10^{-10}	6.674×10^{-10}	6.742×10^{-10}	6.002×10^{-10}
	8	2.462×10^{-09}	2.476×10^{-9}	2.503×10^{-9}	2.195×10^{-9}

Table 14. Corresponding maximum error norm between exact and numerical solution of problem 6 (case 1).

		$\eta = 0.001$		$\eta = 0.0001$		$\eta = 0.00001$	
t	β	Present	(Javidi and Golbabai 2009)	Present	(Javidi and Golbabai 2009)	Present	(Javidi and Golbabai 2009)
0.3	1	3.158×10^{-8}	3.160×10^{-8}	3.161×10^{-10}	3.163×10^{-10}	3.160×10^{-12}	3.163×10^{-12}
	10	3.970×10^{-7}	3.974×10^{-7}	3.972×10^{-9}	3.976×10^{-9}	3.972×10^{-11}	3.976×10^{-11}
	100	5.031×10^{-6}	5.036×10^{-6}	5.034×10^{-8}	5.038×10^{-8}	5.034×10^{-10}	5.039×10^{-10}
0.9	1	3.336×10^{-8}	3.339×10^{-8}	3.337×10^{-10}	3.340×10^{-10}	3.337×10^{-12}	3.341×10^{-12}
	10	4.193×10^{-7}	4.197×10^{-7}	4.195×10^{-9}	4.199×10^{-9}	4.195×10^{-11}	4.199×10^{-11}
	100	5.311×10^{-6}	5.316×10^{-6}	5.317×10^{-8}	5.322×10^{-8}	5.317×10^{-10}	5.322×10^{-10}

4.8. Case 2

Here, we solve the problem in the spatial domain $[-10, 20]$. Computational results are presented for various set of parameters, to check the performance of the technique and also match the results with some existing techniques. We set $\alpha = \beta = \delta = 1$ and $\eta = 2$ for the numerical simulations. In Table 15 the attained maximum error norms are combined for the final time up to $t = 10$. The same table also contains the comparison with the work given in Mittal and Tripathi (2015). Comparison shows that proposed method has better results. In Figure 7, analytical versus approximate solution at different time levels are presented.

5. Computational stability

In this section, the stability region of the present solution strategy is examined using the well-known rule of thumb (Butcher 2007). According to the

Table 15. Calculated maximum error norm between exact and numerical solution of problem 6 (case 2).

t	Present	(Mittal and Tripathi 2015)
0.01	3.076×10^{-7}	2.097×10^{-6}
1	2.092×10^{-5}	9.173×10^{-5}
5	8.768×10^{-4}	1.027×10^{-3}
10	1.206×10^{-4}	1.207×10^{-4}

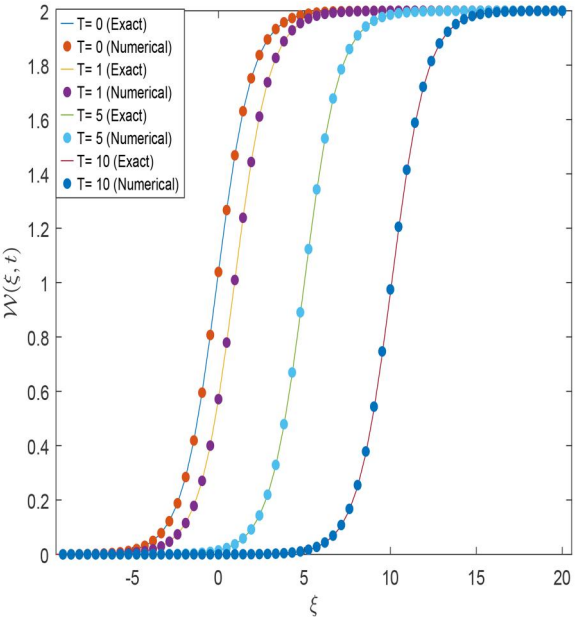

Figure 7. Exact and approximate solution of problem 6 for $\alpha = \beta = \delta = 1$ and $\eta = 2$.

statement of this rule, the computational method will be stable if all the eigenvalues of the discretized linear space operator scaled by the time step ∂t, are located in the stability region of the discretized time operator.

In this work, highly nonlinear gBFE and gBHE are solved numerically. The proposed solution strategy is two steps method, in the first step the spatial part of gBFE and gBHE are discretized by HW series. After the spatial part discretization highly nonlinear system of initial value problems are obtained variable in time only. In the second step the obtained system is solved by RK-4 method. In the stability of the proposed method the jacobian matrix play a crucial role which are described for gBFE and gBHE as:

a. For gBFE: $\Phi_1 = \gamma \mathrm{H} - \alpha(diag(\mathcal{W}(t)))^{\sigma} * \mathrm{S}_1 + \beta(\mathcal{W}(t))^{\sigma}(1 - (\mathcal{W}(t))^{\sigma})$,
b. For generalized gBHE:
$\Phi_1 = \gamma \mathrm{H} - \alpha(diag(\mathcal{W}(t)))^{\sigma} * \mathrm{S}_1 + \beta(\mathcal{W}(t))(1 - (\mathcal{W}(t))^{\sigma})((\mathcal{W}(t))^{\sigma} - \eta)$,

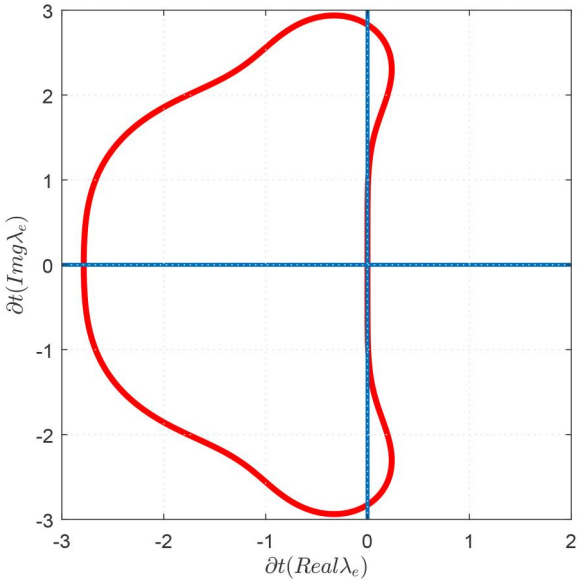

Figure 8. Stability region of RK-4 method.

where, $(diag(\mathcal{W}(t)))^{\sigma} * S_1$ denote the element wise product of $\mathcal{W}(t)$ and square matrix S_1. Stability of the current method depend on the eigenvalues of these matrices which satisfy the stability conditions of the RK-4 method. In the current work the eigenvalues of the Jacobin matrix is complex number obtained from the numerical experiments. The eigenvalues of jacobian matrix and time step size is denoted by λ_e and ∂t respectively. For the stable solution, the following conditions will be ensured:

- For all real eigenvalues the condition holds is $-2.78 < \partial t\lambda_e < 0$
- For all imaginary eigenvalues the condition holds is $-2\sqrt{2} < \partial t \lambda_e < 2\sqrt{2}$
- The complex eigenvalues lie in the stability region of RK-4 method Figure 8.

For different problem, the eigenvalues are computed and plotted in Figures 9–11. Graphically, it is visible that the obtained eigenvalues lie in the stable region of RK-4 method.

6. Conclusions

In this work, a hybrid numerical strategy based on HW and RK-4 has been devised for the analysis of highly nonlinear gBFE and gBHE. Initially in this method, the nonlinear PDEs were transformed the system of nonlinear initial value problems. Then, RK-4 solver has been employed for the

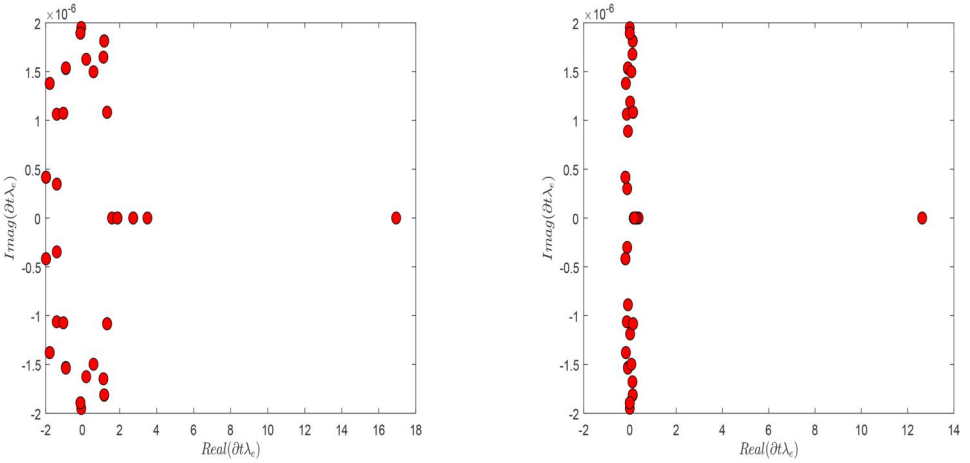

Figure 9. Eigenvalues scattering of Jacobian matrix of problem 1 (left) for $\sigma = 1$ and (right) for $\sigma = 8$ with $t = 0.3$ when $\xi \in [0, 1]$.

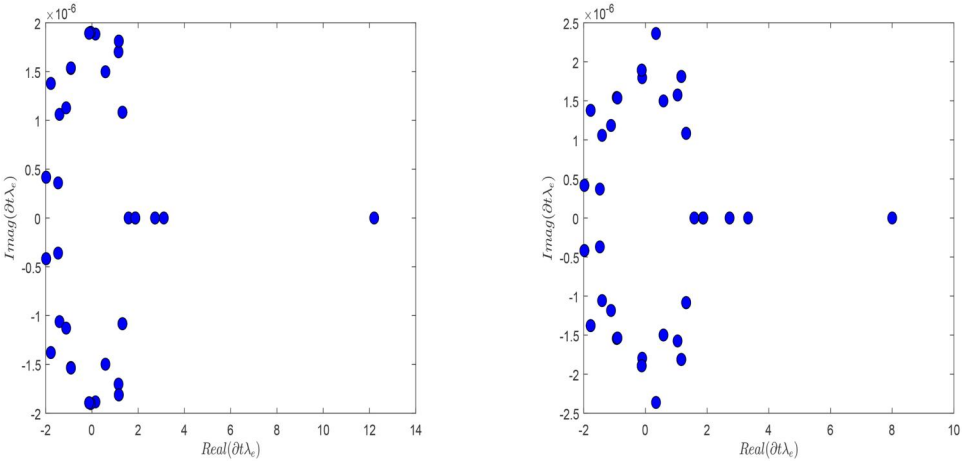

Figure 10. Eigenvalues scattering of Jacobian matrix of problem 2 (left) when $\xi \in [0, 1]$ and (right) when $\xi \in [-10, 10]$ with $t = 0.5$.

solutions of the resultant system. Further, the methods have been applied for the solutions of some nonlinear problems. The accuracy of the method has been evaluated *via* computing various error norms. Besides this, a rigorous comparison with existing work has been conducted which show the superiority of the present method. Moreover, the stability of the scheme has been verified computationally. From computation, we can say that the method is quite feasible for the corresponding nonlinear problems and can be used for such other problems in various branches of science and engineering.

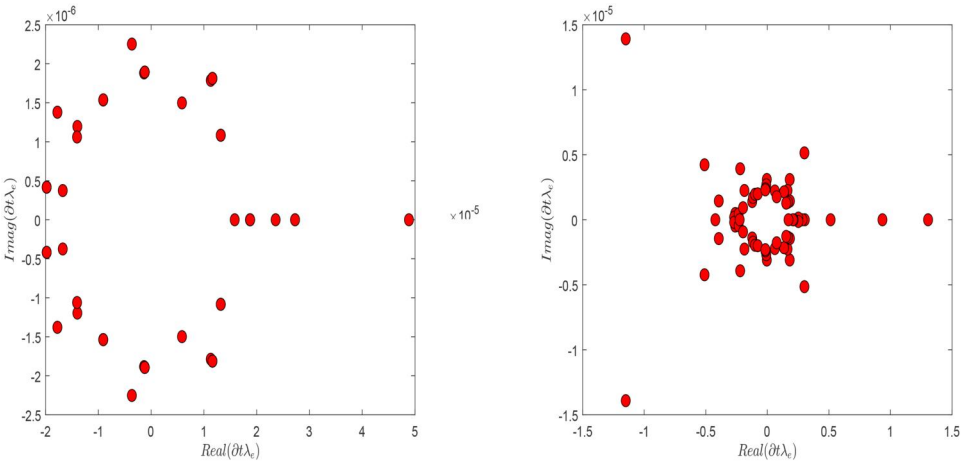

Figure 11. Eigenvalues scattering of Jacobian matrix of problem 6 (left) when $\xi \in [0, 1]$ with $\alpha = 0.1$, $\beta = 0.001$, $eata = 0.0001$ and $\delta = 1$ at $t = 0.5$ and (right) when $\xi \in [-10, 10]$ with $\alpha = \beta = eata = 1$ and $\delta = 2$ at $t = 0.5$.

The current numerical stratagem can be extended to other research directions. In future, this can be applied to handle different nonlinear models that used in fluid dynamics and biological systems, to verify its universal applicability for various nonlinear phenomena. Second, extending this approach to higher-dimensional PDEs could enhace its affectivity in more complex scenarios, such as two and three-dimensional gBFE and gBHE or other higher-dimensional nonlinear problems. The development of new directions, would lead to fruitful progress by broadening numerical solution capabilities for complex PDEs and improving their performance.

Acknowledgements

Authors are thankful to Prince Sultan University for support through TAS research lab. Also, Princess Nourah bint Abdulrahman University Researchers Supporting Project number (PNURSP2025R14), Princess Nourah bint Abdulrahman University, Riyadh, Saudi Arabia.

Author contributions

CRediT: **Aslam Khan**: Methodology, Writing – original draft; **Abdul Ghafoor**: Formal analysis, Supervision, Validation, Writing – review & editing; **Kamal Shah**: Data curation, Project administration; **Thabet Abdeljawad**: Funding acquisition, Investigation; **Manar A. Alqudah**: Funding acquisition, Visualization.

Disclosure statement

No potential conflict of interest was reported by the authors.

Funding

No funding is available.

Data availability statement

The data would be provided on demand.

References

Ablowitz MJ, Fuchssteiner B, Kruskal M. 1987. Topics in soliton theory and exactly solvable nonlinear equations: proceedings of the conference on nonlinear evolution equations, solitons and the inverse scattering transform. World Scientific.

Akinfe TK, Loyinmi AC. 2021. A solitary wave solution to the generalized burgers-fisher's equation using an improved differential transform method: a hybrid scheme approach. Heliyon. 7(5):e07001. https://doi.org/10.1016/j.heliyon.2021.e07001

Ali Shah F, Boulila W, Koubaa A, Mlaiki N, Kamran. 2023. Numerical solution of advection–diffusion equation of fractional order using chebyshev collocation method. Fractal Fract. 7(10):762. https://doi.org/10.3390/fractalfract7100762

Az-Zo'bi EA. 2014. On the reduced differential transform method and its application to the generalized burgers-huxley equation. Appl Math Sci. 8(177):8823–8831.

Bratsos AG. 2011. A fourth order improved numerical scheme for the generalized burgers–huxley equation. AJCM. 01(3):152–158. https://doi.org/10.4236/ajcm.2011.13017

Bratsos AG. 2013. An improved second-order numerical method for the generalized burgers–fisher equation. ANZIAM J. 54(3):181–199.

Butcher J. 2007. Runge-kutta methods. Scholarpedia. 2(9):3147. https://doi.org/10.4249/scholarpedia.3147

Çelik İ. 2012. Haar wavelet method for solving generalized burgers–huxley equation. Arab J Math Sci. 18(1):25–37. https://doi.org/10.1016/j.ajmsc.2011.08.003

Çelik İ. 2016. Chebyshev wavelet collocation method for solving generalized burgers–huxley equation. Math Meth Appl Sci. 39(3):366–377. https://doi.org/10.1002/mma.3487

Darvishi M, Kheybari S, Khani F. 2008. Spectral collocation method and darvishi's preconditionings to solve the generalized burgers–huxley equation. Commun Nonlinear Sci Numer Simul. 13(10):2091–2103. https://doi.org/10.1016/j.cnsns.2007.05.023

Farkov YA, Manchanda P, Siddiqi AH. 2019. Haar–Fourier analysis. In Construction of Wavelets Through Walsh Functions, 79–98, Springer, Berlin.

Fatima N. 2022. Higher order burgers and non linear equation with different boundary condition by hpm. IJMTT. 68(2):133–140. https://doi.org/10.14445/22315373/IJMTT-V68I2P520

Ghafoor A, Haq S, Hussain M, Abdeljawad T, Alqudah MA. 2022. Numerical solutions of variable coefficient higher-order partial differential equations arising in beam models. Entropy. 24(4):567. https://doi.org/10.3390/e24040567

Ghafoor A, Khan N, Hussain M, Ullah R. 2022. A hybrid collocation method for the computational study of multi-term time fractional partial differential equations. Comput Math Appl. 128:130–144. https://doi.org/10.1016/j.camwa.2022.10.005

Haq S, Ghafoor A. 2018. An efficient numerical algorithm for multi-dimensional time dependent partial differential equations. Comput Math Appl. 75(8):2723–2734. https://doi.org/10.1016/j.camwa.2018.01.004

Hussain M, Haq S. 2021. Numerical solutions of strongly non-linear generalized burgers–fisher equation via meshfree spectral technique. Int J Comput Math. 98(9):1727–1748. https://doi.org/10.1080/00207160.2020.1846729

Inan B, Bahadir A. 2015. Numerical solutions of the generalized burgers-huxley equation by implicit exponential finite difference method. J Appl Math Stat Inform. 11(2):57–67.

Javidi M, Golbabai A. 2009. A new domain decomposition algorithm for generalized burger's–huxley equation based on chebyshev polynomials and preconditioning. Chaos, Solitons Fractals. 39(2):849–857. https://doi.org/10.1016/j.chaos.2007.01.099

Javidi M. 2006. Spectral collocation method for the solution of the generalized burger–fisher equation. Appl Math Comput. 174(1):345–352. https://doi.org/10.1016/j.amc.2005.04.084

Kumar H, Yadav N, Nagar AK. 2022. Numerical solution of generalized burger–huxley & huxley's equation using deep galerkin neural network method. Eng Appl Artif Intell. 115:105289. https://doi.org/10.1016/j.engappai.2022.105289

Lepik Ü. 2005. Numerical solution of differential equations using haar wavelets. Math Comput Simul. 68(2):127–143. https://doi.org/10.1016/j.matcom.2004.10.005

Lepik Ü. 2011. Solving pdes with the aid of two-dimensional haar wavelets. Comput Math Appl. 61(7):1873–1879. https://doi.org/10.1016/j.camwa.2011.02.016

Machado J, Babaei A, Moghaddam BP. 2016. Highly accurate scheme for the cauchy problem of the generalized burgers-huxley equation. Acta Polytech Hungar. 13(6):183–195.

Maleknejad K, Lotfi T, Mahdiani K. 2007. Numerical solution of first kind fredholm integral equations with wavelets-galerkin method (WGM) and wavelets precondition. Appl Math Comput. 186(1):794–800. https://doi.org/10.1016/j.amc.2006.08.027

Malik SA, Qureshi IM, Amir M, Malik AN, Haq I. 2015. Numerical solution to generalized burgers'-fisher equation using exp-function method hybridized with heuristic computation. PLoS One. 10(3):e0121728. https://doi.org/10.1371/journal.pone.0121728

Mittal R, Arora G. 2010. Efficient numerical solution of fisher's equation by using b-spline method. Int J Comput Math. 87(13):3039–3051. https://doi.org/10.1080/00207160902878555

Mittal R, Jiwari R. 2009. Numerical study of fisher's equation by using differential quadrature method. Int. J. Inf. Syst. Sci. 5(1):143–160.

Mittal R, Rohila R. 2017. A study of one dimensional nonlinear diffusion equations by bernstein polynomial based differential quadrature method. J Math Chem. 55(2):673–695. https://doi.org/10.1007/s10910-016-0703-y

Mittal R, Tripathi A. 2015. Numerical solutions of generalized burgers–fisher and generalized burgers–huxley equations using collocation of cubic b-splines. Int J Comput Math. 92(5):1053–1077. https://doi.org/10.1080/00207160.2014.920834

Mujahid H and Mehnaz. 2016. Numerical solution of fisher's equation by using meshless method of lines.

Pirdawood MA, Sabawi YA. 2021. High-order solution of generalized burgers–fisher equation using compact finite difference and dirk methods. J Phys Conf Ser. 1999(1):12088. No. IOP Publishing.

Rashidi M, Ganji D, Dinarvand S. 2009. Explicit analytical solutions of the generalized burger and burger–fisher equations by homotopy perturbation method. Numerical Methods Partial. 25(2):409–417. https://doi.org/10.1002/num.20350

Sari M, Gürarslan G, Dağ İ. 2010. A compact finite difference method for the solution of the generalized burgers–fisher equation. Numerical Methods Partial. 26(1):125–134. https://doi.org/10.1002/num.20421

Sari M, Gürarslan G. 2009. Numerical solutions of the generalized burgers-huxley equation by a differential quadrature method. Math Prob Eng. 2009(1):370765. https://doi.org/10.1155/2009/370765

Shiralashetti S, Kumbinarasaiah S. 2018. Cardinal b-spline wavelet based numerical method for the solution of generalized burgers–huxley equation. Int J Appl Comput Math. 4(2): 1–13. https://doi.org/10.1007/s40819-018-0505-y

Singh A, Dahiya S, Singh S. 2020. A fourth-order b-spline collocation method for nonlinear burgers–fisher equation. Math Sci. 14(1):75–85. https://doi.org/10.1007/s40096-019-00317-5

Singh BK, Arora G, Singh MK. 2016. A numerical scheme for the generalized burgers–huxley equation. J Egypt Math Soc. 24(4):629–637. https://doi.org/10.1016/j.joems.2015.11.003

Verma AK, Kayenat S. 2020. An efficient mickens' type nsfd scheme for the generalized burgers huxley equation. J Diff Eq Appl. 26(9-10):1213–1246. https://doi.org/10.1080/10236198.2020.1812594

Wasim I, Abbas M, Amin M. 2018. Hybrid b-spline collocation method for solving the generalized burgers-fisher and burgers-huxley equations. Math Prob Eng. 2018:1–18. https://doi.org/10.1155/2018/6143934

Xu Z-h, Xian D-q 2010. Application of exp-function method to generalized burgers-fisher equation. Acta Math Appl Sin Engl Ser. 26(4):669–676. https://doi.org/10.1007/s10255-010-0031-0

Zaman SS, Amin R, Haider N, Aloqaily A, Mlaiki N. 2024. Haar wavelet collocation technique for numerical solution of porous media equations. Partial Diff Eq Appl Math. 10: 100728. https://doi.org/10.1016/j.padiff.2024.100728

Zhao T, Li C, Zang Z, Wu Y. 2012. Chebyshev–legendre pseudo-spectral method for the generalised burgers–fisher equation. Appl Math Modell. 36(3):1046–1056. https://doi.org/10.1016/j.apm.2011.07.059

Zhu C-G, Kang W-S. 2010. Numerical solution of burgers–fisher equation by cubic b-spline quasi-interpolation. Appl Math Comput. 216(9):2679–2686. https://doi.org/10.1016/j.amc.2010.03.113